Generating high node congruence in freeform structures with Monge's Surfaces

Romain Mesnil, Yann Santerre, Cyril Douthe, Olivier Baverel, Bruno Leger

Proceedings of the International Association for Shell and Spatial Structures (IASS)
Symposium 2015, Amsterdam
Future Visions
17 - 20 August 2015, Amsterdam, The Netherlands

Generating high node congruence in freeform structures with Monge's Surfaces

Romain MESNIL*[a,b], Yann SANTERRE[a], Cyril DOUTHE[a],
Olivier BAVEREL[a], Bruno LEGER[b]

* [a] Université Paris Est, Laboratoire Navier
romain.mesnil@enpc.fr
[b] Bouygues Construction SA, FRANCE

Abstract

The repetition of elements in a free-form structure is an important topic for the cost rationalization process of complex projects. Although nodes are identified as a major cost factor is steel grid shells, little research has been done on node repetition. This paper proposes a family of shapes, called isogonal moulding surfaces, having high node congruence, flat panels and torsion-free nodes. It is shown that their generalization, called Monge's surfaces, can be approximated by surfaces of revolution, yielding high congruence of nodes, panels and members. These shapes are therefore interesting tools for geometrically-constrained design approach.

Keywords: conceptual design, structural morphology, fabrication-aware design, moulding surfaces, rationalization

1. Introduction

Complex shapes play an increasing role in contemporary architecture. Recent developments in digital fabrication and modeling or representation techniques have allowed new formal possibilities. The rationalization of these new shapes is an important issue, which has led to a significant research effort in the field of discrete differential geometry.

Geometrical optimization generally considers two aspects: geometry of panels and the geometry of structures. Flat quadrangular panels have been identified as a very efficient solution to the panelization problem by (Schlaich and Schober [12], Glymph *et al.* [3]). Another typical geometrical optimization task is to find discrete normal to nodes, such as the one displayed on Figure 1, and to have planar beams spanning between them. Meshes that admit such offsets are called conical meshes and were introduced in (Liu *et al.* [5]). Optimization towards planar conical meshes is possible only when the mesh is aligned with the lines of curvature of the surface to cover. Current methods require integration of vector fields, which lacks flexibility in the early steps of design, as it cannot be realized in real-time and can yield unpredictable results on the topology of curvature lines (Wallner and Pottmann [14]). The objective of optimization towards planar conical meshes can be restricted to

constant-edge offset: in this case, constant height beams are perfectly aligned on the top and bottom of each node. Meshes satisfying this property are called *Edge Offset Meshes*, and they are related to very specific surfaces (Pottmann *et al.* [11]). The modeling of complex shapes as Edge Offset Mesh is still a challenge for designers.

Repetition of elements is also of importance in the cost-reduction process. Repetition of members length in free-form structures has been explored for applications to elastic grid shells very early, and is still and active reseach topic (Otto [10], Bouhaya *et al.* [2]). The topic of repetition has also been studied for the repetition of panels, for example with clustering techniques (Eigensatz *et al.* [4]). However, although connections are identified as a major cost factor in steel grid shells, little research has been done on node-repetition in free-form structures.

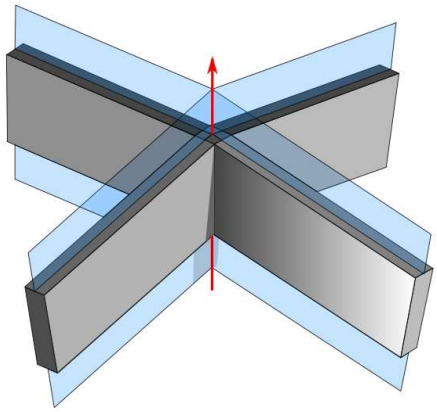

Figure 1: A torsion-free node: planes of symmetry of beams meet along a common line

This paper proposes a family of shapes that can naturally be described as planar conical meshes, with high node congruence, and possible optimization towards Edge Offset Meshes. This restriction of the formal possibilities guarantees that the final shape can easily be constructed. This paper also studies Monge's surfaces, and shows that the number of different nodes, panels or members can be optimized.

Main contributions of this paper include:

- Description of a new family of surfaces with high node congruence and planar quadrilateral conical mesh: isogonal moulding surfaces.
- Practical tools to mesh isogonal moulding surfaces with perfect nodes.
- Approximation of Monge's surfaces with patches of surface of revolution, which yields high repetition of members, panels, and nodes.

This paper is organised as follows: Section 2 discusses the generation and properties of isogonal moulding surfaces and of Monge's surfaces. The numerical implementation together with some case studies is presented in Section 3. An extension of the results obtained for isogonal moulding surfaces is proposed for Monge's surfaces in Section 4.

2. Isogonal moulding surfaces

2.1. Monge's surfaces

Monge's surfaces, or generalized moulding surfaces, are a subset of sweeping sufaces first studied by Gaspard Monge in (Monge [8]). They are generated by the sweeping of curve, called generatrix (in orange on *Figure 2*) along a rail curve also called parallel (in blue on *Figure 2*). The restriction to apply is that the swept curve has to lie initially within the normal plane of the rail curve, and it has to follow the *rotation-minimizing frame*.

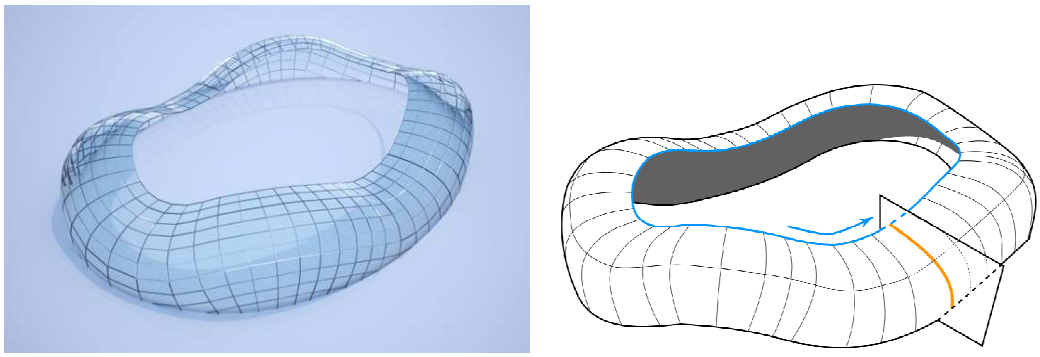

Figure 2: Stadium as a Monge's surface

2.2. Isogonal moulding surfaces

Moulding surfaces were introduced by Gaspard Monge as a restriction of Monge's surfaces: the parallels of moulding surfaces are necessarily planar. An interesting subset of moulding is made of surfaces where the rail is subdivided with a constant angle. Such surfaces are called isogonal moulding surfaces (Mesnil *et al.* [6]).

These surfaces have interesting congruence properties for nodes. Namely, all the nodes belonging to the same parallel of a moulding surface are congruent. In the barrel vault displayed on Figure 3, there are 700 nodes but only 8 types of nodes because the surface is an isogonal moulding surface. Other symmetries can be used to decrease the total number of nodes.

It has been demonstrated in (Mesnil *et al.* [6]) that discrete Monge's surfaces are covered with trapezoids, and that isogonal moulding surfaces are covered with isosceles trapezoids. This has two consequences:

- All the members between two parallels are identical (same length, same angle with the discrete normal). Isogonal moulding surfaces have high member congruence in addition to high node congruence.
- Isogonal moulding surfaces naturally form circular meshes, they can be used as base mesh for generalized cyclidic nets and can be deformed by inversions (Mesnil *et al.* [7]).

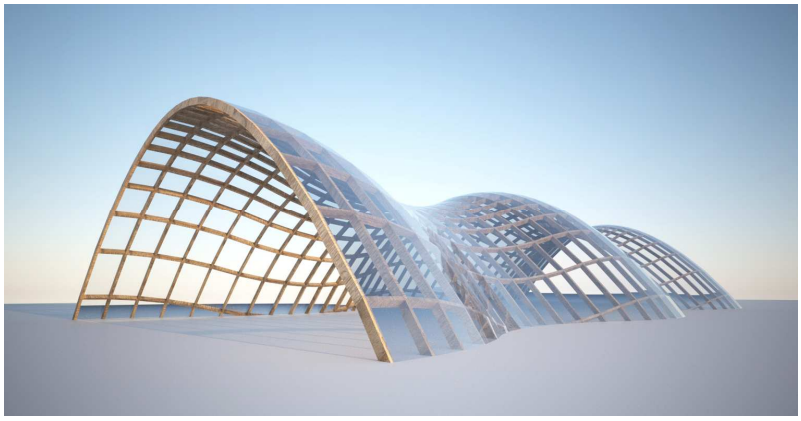

Figure 3: Barrel vault as isogonal moulding surface

2.3. Relation with surfaces of revolution

The high node congruence in isogonal moulding surfaces can be linked to the symmetries observed in surfaces of revolution with one tool: mesh parallelism. A definition of this notion is recalled in (Liu *et al.* [5]): "two meshes are parallel if all their edges are parallel to each other". A transformation of a given mesh to a parallel mesh is called a *Combescure transform*. As angles between edges are preserved by parallelism, a simple corollary is that parallel meshes have identical nodes.

It can be noticed that mesh parallels to discrete moulding surface are discrete moulding surfaces: the parallels remain obviously parallels after a Combescure transform. Even more specifically, mesh parallels to isogonal moulding surfaces are isogonal moulding surfaces because the angle subdivision of parallels is preserved by mesh parallelism.

A surface of revolution is a specific case of moulding surface, where rails are circles. A canonical surface of revolution (with a uniform subdivision of the rail) is therefore an isogonal moulding surface. This demonstrates an important statement, which is illustrated in *Figure 4*: *'All the possible shapes parallels to discrete surfaces of revolution are isogonal moulding surfaces'*.

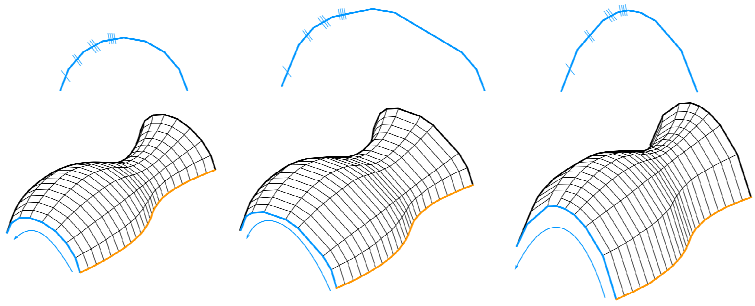

Figure 4: A surface of revolution and two parallel isogonal moulding surfaces

3. Numerical implementation

3.1. Isogonal curve

The main challenge in the design of isogonal moulding surfaces is the isogonal subdivision of the rail curve. A generic algorithm is proposed and described in (Mesnil et al. [6]), it has a simple graphical counterpart illustrated in Figure 5. The algorithm can be described as follows:

1. Find the tangent vectors $\mathbf{T}_A$ and $\mathbf{T}_B$ at the ends of the curve, and measure their angle α_{AB}. If the curve is closed and convex, chose $\alpha_{AB} = 2\,\pi$.
2. Divide α_{AB} by the number **n** of inner nodes. Create the vectors ($\mathbf{T}_i$) with i in [1, n-1] , where each $\mathbf{T}_i$ is obtained by a rotation of $\mathbf{T}_A$ by an angle of (i. α_{AB} /n).
3. Find the points corresponding to the tangency to the ($\mathbf{T}_i$) on the initial curve.
4. Intersect the corresponding lines with each other.

The algorithm has been implemented within Grasshopper and requires less than 200ms for a hundred subdivisions. This guarantees a real-time visualization and generation of isogonal moulding surfaces.

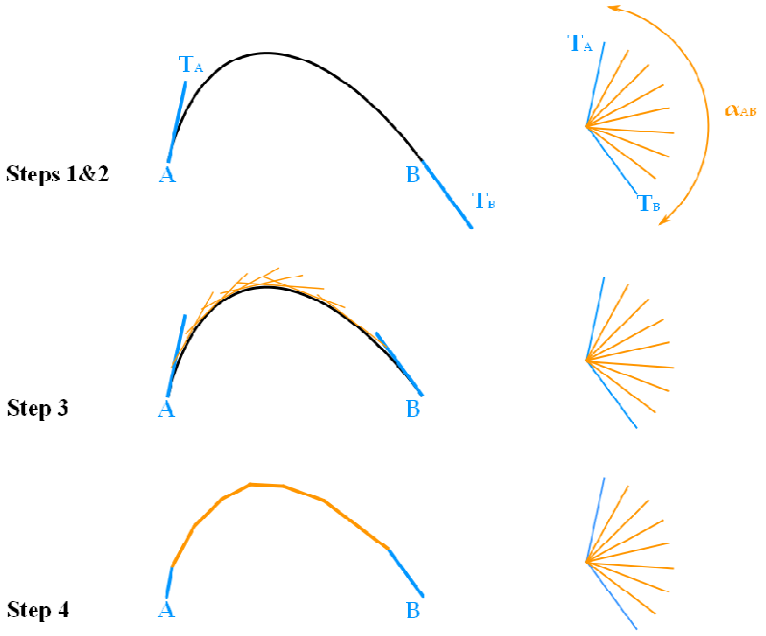

Figure 5: Graphical method for an isogonal subdivision of a planar curve

3.2. Edge Offset Meshes and moulding surfaces

Edge Offset Meshes on moulding surfaces are related to Koebe Meshes with a rotational symmetry. In order to cover moulding surfaces with perfect nodes, it is necessary to compute the equivalent Koebe

Mesh, i.e. a circle packing on the sphere with a rotational symmetry. They are only two circles that are tangent with two meridians (red lines on *Figure 6*) and a given parallel (blue dotted lines on *Figure 6*). Mathematically, this means that one value of the latitude λ_i defines two possible values of λ_{i+1} that guarantee the construction of a circle packing with rotational symmetry.

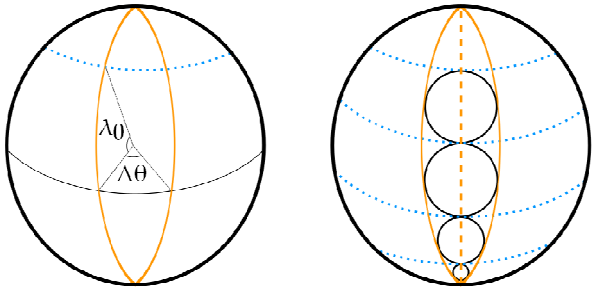

Figure 6: Koebe Mesh with rotational symmetry, parallels (blue dotted lines) and meridians (red plain lines)

The problem thus depends only on the latitude of the tangency point on the sphere λ_i and of the rail subdivision angle $\Delta\theta$. Introducing $t_i = \tan \lambda_i / 2$ and the constant $K_\theta = 1 + 2\sin^2 \Delta\theta / 2$, the solution follows:

$$t_{i+1} = \frac{2t_i \pm \left(1 - {t_i}^2\right)\sqrt{1 - {K_\theta}^2}}{\left(1 - K_\theta\right){t_i}^2 + \left(1 + K_\theta\right)} \tag{1}$$

The plus or minus sign depends whether the mesh is propagated towards the North Pole or the South Pole. The values of interest on the targeted moulding surface are two parameters that are conserved by Combescure transform: the rail subdivision angle α_i, and the angle of each section of the meridian in the discrete Frénet frame of the rail β_j, as seen on Figure 7. Once the angles λ_j are retrieved from the Koebe Mesh, it is possible to construct the angles β_j for the Koebe Mesh and the moulding surface.

The computation is fast (200ms for 1000 faces), and guarantees an efficient exploration of the possible shapes of Edge Offset Mesh on isogonal moulding surfaces. Some examples of domes as Edge Offset Meshes are shown on Figure 8. It appears that the aspect ratio of the panels (length over width) corresponds to the ratio of principal curvatures. On Figure 8, the dome on the left has a strong curvature anisotropy and an important aspect ratio on the equivalent Edge Offset Mesh; the dome on the right has a more even distribution of curvatures and, as a result, the equivalent Edge Offset Mesh is more balanced.

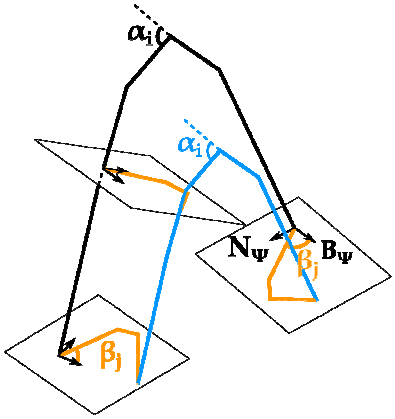

Figure 7: Parameters describing the geometry of a node in an isogonal moulding surface

The main restriction in the design with Edge Offset Meshes is the curvature anisotropy on the target surface, as the shape of the panels cannot be chosen be the designer. The algorithm proposed here does not work for surfaces with zero Gaussian curvature, but performs very well for shapes like domes or barrel vaults.

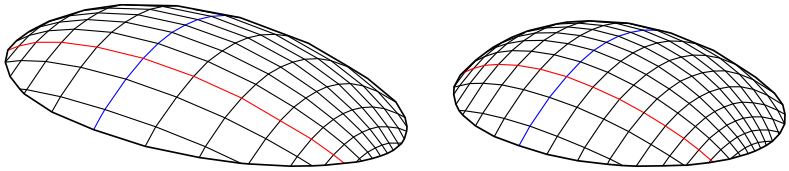

Figure 8: Domes as isogonal moulding surfaces with perfect nodes

4. Toric Monge's surfaces

4.1. Congruence in Monge's surfaces

Isogonal moulding surfaces are proven to be very similar to rotational surfaces, and they inherit some of their congruence properties. Despite their similarities with moulding surfaces, Monge's surfaces do not have such properties in the most general case. This paper proposes to approximate the rail curve and the generatrix by circular arcs. The sweeping of a circle along a circle represent a portion of torus, which implies that Monge's surfaces resulting from the sweeping of circulars splines are a concatenation of toric patches. The authors call *toric Monge's surfaces* such surfaces.

Since the resulting surface has a local rotational symmetry, discretization of toric Monge's surfaces have high node congruence, as well as members and panels congruence on each patch. This process can be applied to Monge's surfaces or moulding surfaces, like the one displayed on Figure 9 where the rail curve is approached by three circular arcs. An isogonal moulding surface based on this geometry has panel congruence and not only node congruence.

The congruence increases as the number of patches decreases, it is therefore important to approximate a given curve with as little patches as possible. This motivates the implementation of an optimization algorithm that allows approximation of a given curve with a minimum amount of circular arcs.

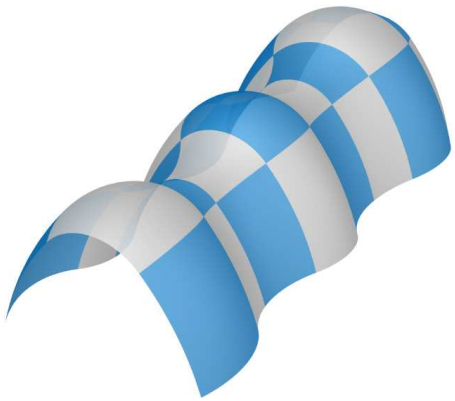

Figure 9: Barrel Vault as a Toric Monge's Surface

4.2. Algorithm principle: bi-arcs

The approximation of a given set of points by circular splines has already been used in architecture and other fields of computer-aided design (Bo *et al.* [1], Song *et al.* [13]). The aforementioned papers use the fact that two prescribed points and two tangent vectors admit a one-parameter family of bi-arcs (two circular arcs), like the one represented on Figure 10.

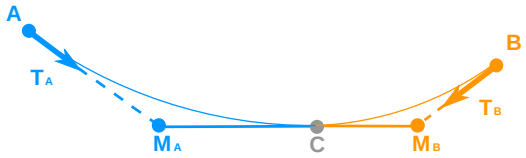

Figure 10 : A biarc and the associated notations

Circular arcs are here described as Non Rational Bézier curves of degree 2. Only three control points are required, one at each end, and one on the line sector bissector. Consider a bi-arc with prescribed points A and B and prescribed tangents T_A and T_B. The two arcs are meeting tangentially at point C following an unknown vector T_C. The control points M_A and M_B are at the intersection of the lines (C,T_C) and (A,T_A) or (B,T_B) respectively. They are defined by the equation:

$$\begin{cases} \mathbf{M_A} = A + l_A \mathbf{T_A} \\ \mathbf{M_B} = B + l_B \mathbf{T_B} \end{cases} \tag{2}$$

The two arcs meet tangentially, meaning that M_A, M_B and C are aligned:

$$\left\|\mathbf{M_A} - \mathbf{M_B}\right\|^2 = \left(l_A + l_B\right)^2 \tag{3}$$

Equations (2) and (3) lead to an equation with two unknowns that any bi-arc has to satisfy the equation (4), found in (Song *et al.* [13]):

$$\mathbf{V^T V} + 2l_A\mathbf{V T_A} + 2l_B\mathbf{V^T T_B} + 2l_A l_B\left(\mathbf{T_A T_B} - 1\right) = 0 \tag{4}$$

where $\mathbf{V} = B - A$. This equation has an infinity of solutions. It can be transformed into a parametric equation, for example by introducing the parameter $r = \frac{l_A}{l_B}$. The equation becomes then a second order polynomial equation in l_A, which has one positive solution for any value of *r*.

4.2.1. Parameters

Two points and two tangent vectors give a one-parameter family of bi-arcs. In this paper, a set of points is chosen on the curve to approximate. The associated tangent vectors are the tangent vectors of the curve. The approximation of the curve is the set of bi-arcs generated on each set of consecutive points of the curve. The parameters of the problems are therefore the U-values of the points on the curve and the ratio *r* for each bi-arc. For N bi-arcs, there are therefore (N-1) values for (U_i), and N values for (r_i).

4.2.2. Error functional

Section 4.2.1 shows how to generate a N-parameter family of circular splines approaching a reference curve. The question of the estimation of the similarity between two curves remains. A naïve approach would be to minimize the Euclidean distance, but two curves can be close in terms of Euclidean distance and have very different features, as illustrated in Figure 11. When dealing with free-form curves, it is more important to preserve some key visual references, like peaks and valleys. Mathematically, this means that the criterion has to compare the orientations of the normal vectors, as illustrated in Figure 11: this kind of measure validates the fact that the two curves on the right have one unique peak.

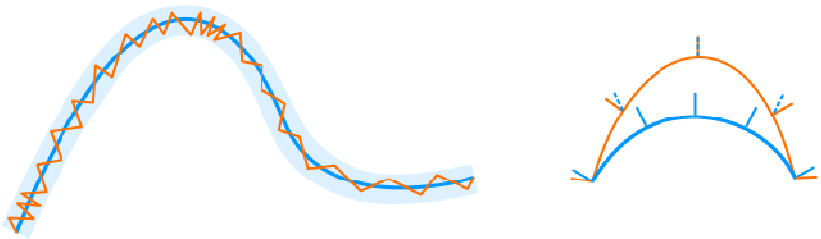

Figure 11: Two curves with a reasonable Euclidean distance but that are visually different (left) and the chosen criterion to assess curves proximity (right)

The functional has the form:

$$E(U,R) = \sum_{biarcs} \int \left\| \vec{n}(s) \times \overrightarrow{n_0}(P') \right\|^2 ds \tag{4}$$

Where *s* is the arc length parameter on the bi-arc, P' is the closest point evaluated on the reference curve and $n_0(P')$ the associated normal vector. The functional penalizes changes of curve inflection and gives satisfactory results. The integrals are computed numerically as finite sums.

$$E(U,R) = \sum_{biarcs} \sum_{1<i<N} l_i \left\| \vec{n}(P_i) \times \overrightarrow{n_0}(P_i') \right\|^2 \tag{5}$$

The number of sampling points is chosen so that the estimation does not vary by more than 0.1% when doubling its value. With the curves studied in this paper, this led to values between 10 and 20 sampling points.

4.2.3. Optimisation

The optimization problem is an unconstrained smooth problem, which hints the use of descent algorithm. The error functional is minimized by a quasi-Newton scheme: the BFGS method. This method computes an approximate value for the Hessian matrix based only on the estimation of the gradient. The method is easy to implement and has a good convergence: it is one of the most popular quasi-Newton methods (Nocedal and Wright [9]).

Once the descent direction is found, it is necessary to find

The optimization is proven to require

4.3. Application

The optimization algorithm has been applied to the rail curve of Monge's surface displayed on Figure 2. The curve is non-planar and has numerous inflection points, but it has a double symmetry. Therefore, only an even number of bi-arcs are used. As the number of bi-arcs increases, the curve becomes more and more similar to the reference curve, as seen on Figure 12. However, this also increases the number of different nodes, or panels when a Monge's surface is generated.

	Reference Surface	**16 Arcs**	**12 Arcs**	**8 Arcs**
Number of families of panels	200	70	50	30
Number of families of nodes	200	40	30	20
Number of families of generatrix	20	4	3	2

Table 1: Repetition of elements in Monge's surface

This aspect of repetition of elements is explored in Table 1, for a subdivision with 80 elements on the rail and 10 elements on the generatrix. The formula for the number of families of elements is given in equations (5) and (6):

$$N_{panels} = n_{generatrix}.(2n_{arcs} - 1) \quad (5)$$

$$N_{nodes} = n_{generatrix}.n_{arcs} \quad (6)$$

In this case-study, the symmetry decreases further the number of different elements. Finally, the high congruence of lengths in isogonal moulding surfaces means that there a lot of identical generatrix in toric Monge's surfaces. This is of particular interest when the main structural elements are along the generatrix, like in stadium design.

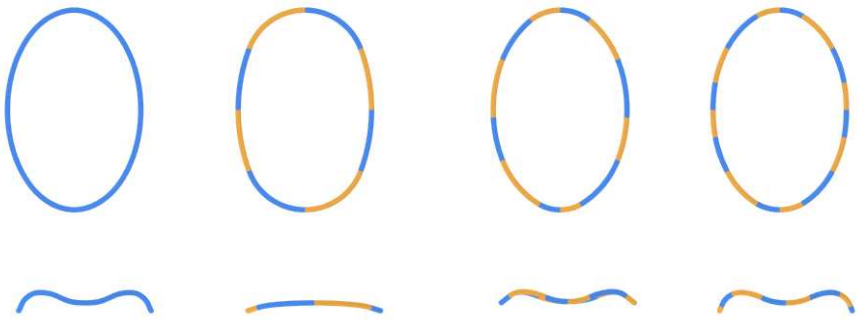

Figure 12: Reference Curve and approximation by 8,12 and 16 arcs: top view, elevation

This case study shows that optimization of Monge's surfaces or moulding surfaces towards concatenation of surfaces of revolution is well performed by the algorithm proposed in this paper. The algorithm reached convergence (variation of the error functional of less than 0.1%) in less than 100ms, which allows real-time manipulation.

5. Conclusion

The construction of complex structures is subject to strong geometrical constraints. In steel grid shell, the cost of connections is proven to be a major factor for the total cost. This paper explored a particular set of surfaces, called isogonal moulding surfaces, that have high node congruence and that are optimal with respect to common optimization targets. It also showed how to cover these surfaces with constant edge offset meshes, and gave hindsight on the potential and practical limitations of such meshes. Finally, this paper presented an algorithm that approximates Monge's surfaces with toric patches; this solution leads to natural covering with planar panels and torsion free nodes together with panels, beams and node repetition. Although this restricts the formal possibilities compared to more general approaches, it describes archetypal shapes of architecture, such as domes, doubly curved barrel vaults, or stadia.

This solution is a particular subset of generalized cyclidic nets, presented in (Mesnil *et al.* [7]). The formal potential of Monge's surfaces could be expanded with Möbius transforms, with a loss of repetition of its elements.

The toric-approximation algorithm introduced in this paper is a descent algorithm, meaning that the initial configuration has an influence on the final outcome. It could be easily combined with genetic algorithms to find a global optimum for the approximation problem.

Acknowledgement

The authors thank the ANRT and Bouygues Construction which financially support this research.

References

[1] Bo P., Pottmann H., Killian M., Wang W., Wallner J., Circular Arc Structures, in *ACM Transactions on Graphics*, 2011; **30**(4):101-111.

[2] Bouhaya L., Baverel O., Caron J.-F., Optimization of gridshell bar orientation using a simplified genetic approach. *Structural and Multidisciplinary Optimization*, 2014; **50**(5);839-848

[3] Glymph J., Shelden D., Ceccato C., Mussel J., Schober H., A parametric strategy for free-form glass structures using quadrilateral planar facets. *Automation in Construction*, 2004;**13**: 187-202.

[4] Eigensatz, M., Deuss, M., Schiftner, A., Kilian, M., Mitra, N. J., Pottmann, H., & Pauly, M., Case studies in cost-optimized paneling of architectural freeform surfaces. in *Advances in Architectural Geometry 2010*, 49-72.

[5] Liu Y., Pottmann H., Wallner J., Yang Y.-L., Wang W., Geometric Modeling with Conical Meshes and Developable Surfaces, in *ACM Transactions on Graphics*, 2006; **25**: 681-689.

[6] Mesnil R., Douthe C., Baverel O., Léger B., Caron J.-F., Isogonal moulding surfaces: a family of shapes for high node congruence in free-form structures. *Automation in Construction*, 2015 (acecpted).

[7] Mesnil R., Douthe C., Baverel O., Léger B., Möbius Geometry and Cyclidic Nets: a framework for complex shape generation, in *IASS 2015 Symposium,Future Visions* (submitted)

[8] Monge G., Application de l'analyse à la géométrie, à l'usage de l'Ecole impériale Polytechnique, (1807).

[9] Nocedal J. and Wright S.J., *Numerical Optimisation*, Springer-Verlag, 2006.

[10] Otto F. IL10 Gitterschalen. Institut für leichte Flächentragwerke (IL), 1974.

[11] Pottmann H., Liu Y., Wallner J., Bobenko A. and Wang W., Geometry of Multi-layer support structures for architecture, in *ACM Transactions on Graphics*, 2007; **26**(3).

[12] Schlaich J., Schober, H., Glass Roof for the Hippo Zoo at Berlin. *Structural Engineering International*, 1997; **7**(4): 252-254

[13] Song X., Aigner M., Chen F and Jüttler B., Circular spline fitting using an evolution process. *Journal of Computational and Applied Mathematics*, 2009; **231**(1): 423-433.

[14] Wallner, J., & Pottmann, H., Geometric computing for freeform architecture. *Journal of Mathematics in Industry*, 2011; **1**(1), 1-19.